

Figure S1. (a) N₂ adsorption (filled points) and desorption (unfilled points) isotherms of Ru/SiO₂(C100) (○), Ru/SiO₂(SC700) (△), Ru/SiO₂(SC800) (▽), Ru/SiO₂(SC900) (☆), Ru/SiO₂(SC930) (□), and Ru/SiO₂(SC950) (◇) and (b) N₂ adsorption (filled points) and desorption (unfilled points) isotherms of Ru/SiO₂(C100) (○), Ru/SiO₂(C300) (△), Ru/SiO₂(C500) (▽), Ru/SiO₂(C700) (☆).

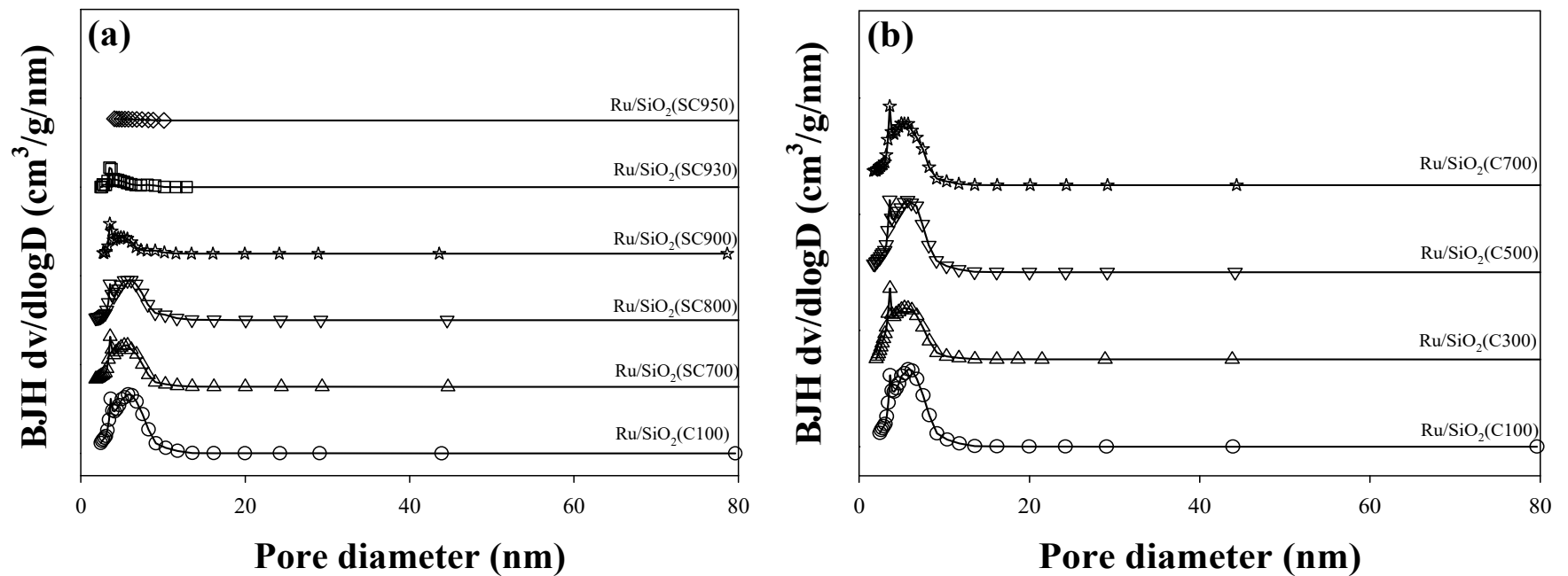


Figure S2. (a) Pore size distribution of Ru/SiO₂(C100) (○), Ru/SiO₂(SC700) (△), Ru/SiO₂(SC800) (▽), Ru/SiO₂(SC900) (☆), Ru/SiO₂(SC930) (□), and Ru/SiO₂(SC950) (◇) and (b) pore size distribution of Ru/SiO₂(C100) (○), Ru/SiO₂(C300) (△), Ru/SiO₂(C500) (▽), Ru/SiO₂(C700) (☆).

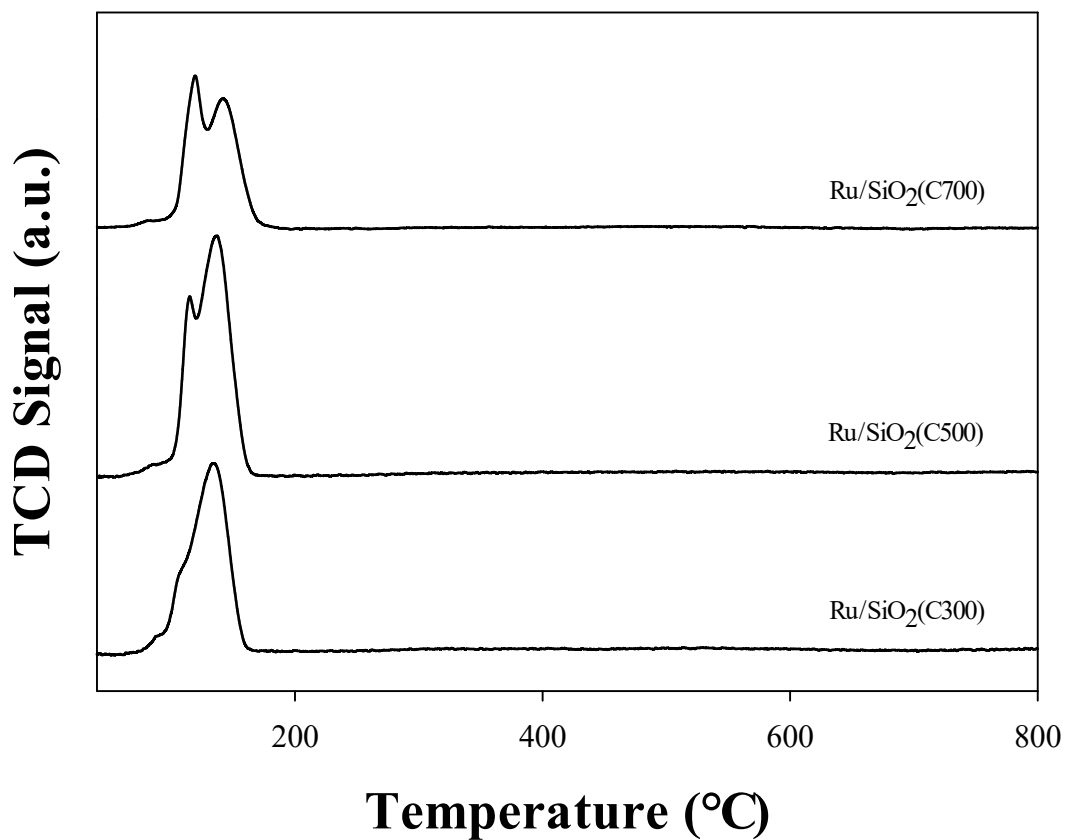


Figure S3. Temperature programmed reduction with H₂ (H₂-TPR) patterns of Ru/SiO₂ calcined at different temperatures such as Ru/SiO₂(C300), Ru/SiO₂(C500), and Ru/SiO₂(C700).

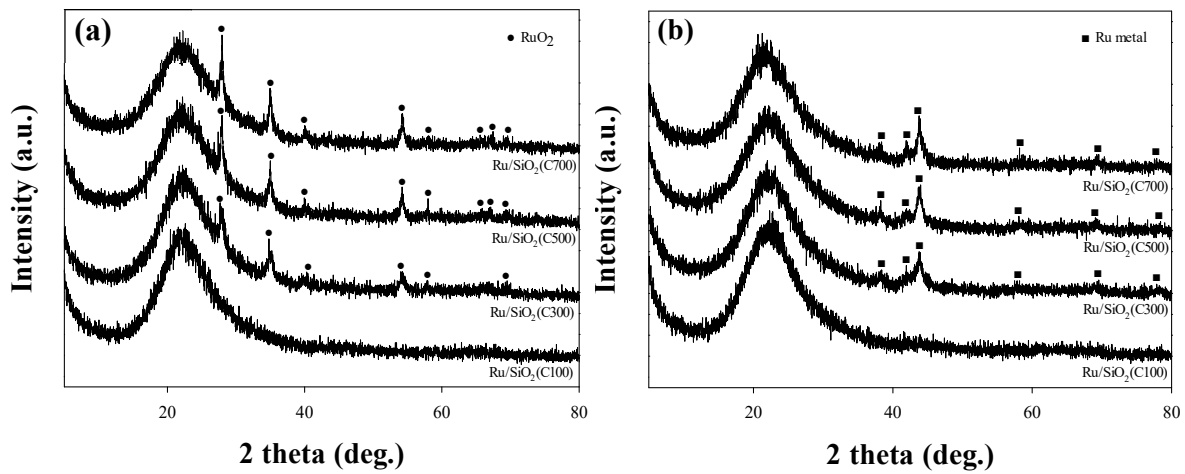


Figure S4. X-ray diffraction (XRD) patterns for Ru/SiO₂ catalysts calcined at different temperatures (a) and Ru/SiO₂ catalysts calcined at different temperatures and then reduced with H₂ at 350 °C (b).

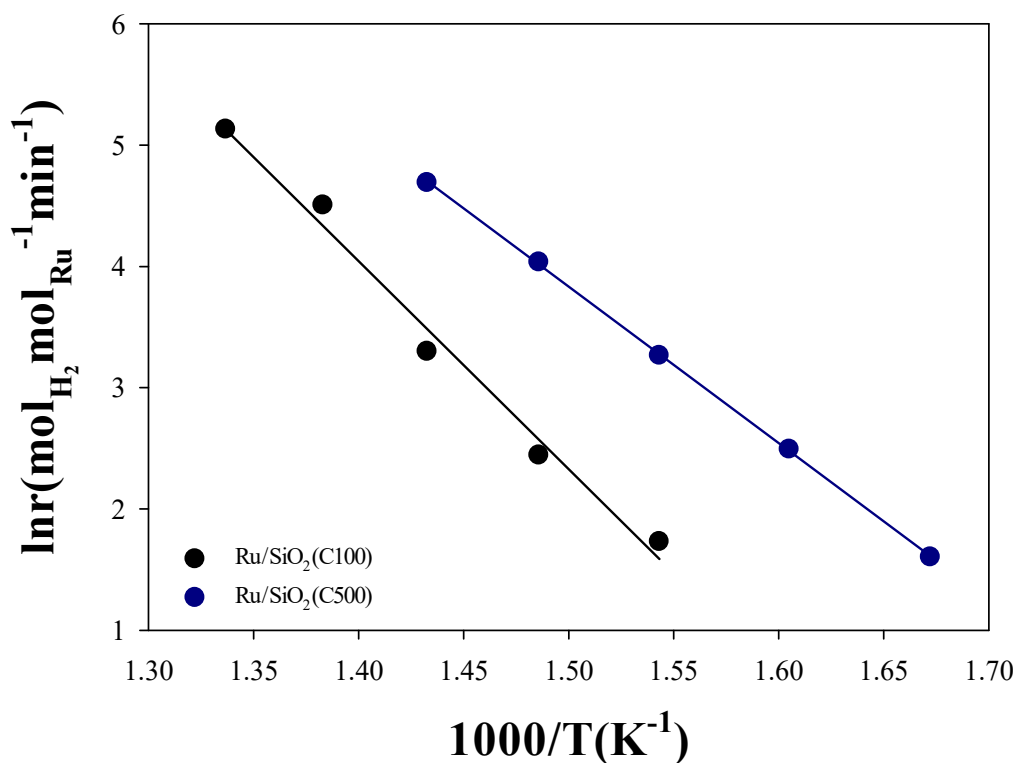


Figure S5. Arrhenius plot for ammonia decomposition over Ru/SiO₂(C100) and Ru/SiO₂(C500).